Submitted to

XXII International Symposium on Lepton-Photon Interactions at High Energy, LP2005
June 30, 2005, Uppsala
Abstract: **400**
Session: **QCD and hadron structure**

www-h1.desy.de/h1/www/publications/conf/conf_list.html

Search for the Strange Pentaquark Θ^+ Decaying to $K^0_S p$ with the H1 Detector at HERA

H1 Collaboration

Abstract

Recently observations of a narrow baryonic state decaying to charged kaons and neutrons or K^0_s mesons and protons have been reported by several experiments. This resonance could be identified as a candidate for the exotic Θ^+ pentaquark state. Preliminary results from the H1 experiment on the search for the production of the Θ^+ and its antiparticle in the invariant mass combinations of K^0_s mesons with protons and antiprotons in deep-inelastic ep-scattering at HERA are presented. The invariant $K^0_s p$ mass distribution does not show any significant signal in the mass range from threshold up to 1.7 GeV/c^2. Assuming pentaquarks to be produced in fragmentation upper limits on the visible $\Theta^\pm$ production cross section are obtained for different kinematic regions.

1 Introduction

Recently several experiments have published evidence for the production of a strange pentaquark Θ^+ by various reaction processes [1, 2, 3]. It has been observed via its decays into K^+n and into K_s^0p. Positive evidence for the production of Θ^+ has also been obtained in deep-inelastic ep-scattering at HERA [3] which may suggest pentaquark formation as part of fragmentation in high energy processes. Negative preliminary results, however, have been reported [4] from pp and ep collisions, e^+e^- annihilation and also from fixed target photo-production experiments.

Several theoretical models [5] have predicted mass spectra for the pentaquark multiplets but currently there is almost no understanding of the production mechanism of these exotic baryons in high energy experiments. Therefore it is difficult to draw any conclusions from the experimentally controversal situation of observation and non-observation results of such states.

Preliminary results on the search for the strange pentaquark Θ^+ decaying into K_s^0p in deep inelastic ep scattering with the H1 detector are presented here. Despite of the ignorance of the pentaquark production mechanism in high energy processes it is assumed that pentaquark formation is part of the fragmentation process as supported by [3] and by [6] for the strange and the charmed pentaquark, respectively. Within this model upper limits are derived on the visible Θ^+ cross section in deep inelastic ep scattering at HERA.

2 Experimental Procedure

2.1 H1 Apparatus

The tracks from charged particles used in this analysis are reconstructed in the H1 central tracker, whose main components are two cylindrical drift chambers, the inner and outer central jet chambers (CJCs), covering the polar angle region $20^\circ < \theta < 160^\circ$. The H1 experiment uses a coordinate system in which the positive z-axis is defined by the direction of the outgoing proton beam. The polar angle θ of a particle is defined relative to this axis and is related to the pseudorapidity η by $\eta = -\ln\tan\theta/2$. The inner and outer CJCs are mounted concentrically around the beam-line, have 24 and 32 sense wires, respectively, and cover radii between 20 cm and 84 cm. The information from the CJC sense wires is digitised using 100 MHz FADCs, providing simultaneous charge and timing measurements. The CJCs lie within a homogeneous magnetic field of 1.15 T, which allows measurements of the transverse momenta of charged particles. Two additional drift chambers complement the CJCs by precisely measuring the z coordinates of track segments and hence assist in the determination of the particle's polar angle. The Central Silicon Tracker, consisting of two layers at radii of 6 cm and 10 cm, is also used to improve the charged particle track and event vertex reconstruction. The transverse momentum resolution of the central tracker is $\sigma(p_{\rm T})/p_{\rm T} \simeq 0.005\, p_{\rm T}$ [GeV] $\oplus 0.015$. The charge misidentification probability is negligible for particles originating from the primary vertex which have transverse momenta in the range relevant to this analysis.

The specific ionisation energy loss of charged particles is derived from the mean of the inverse square-root of the charge collected by all CJC sense wires with a signal above threshold. The resolution is $\sigma(\mathrm{d}E/\mathrm{d}x)/(\mathrm{d}E/\mathrm{d}x) \simeq 8\%$ on average for minimum ionising particles [7].

A lead/scintillating-fibre spaghetti calorimeter (SpaCal) is located in the direction of the outgoing electron beam. It contains both electromagnetic and hadronic sections and is used to detect the scattered electron in DIS events. The global properties of the hadronic final state are reconstructed using an algorithm which takes information from the central tracker, the SpaCal, and also from a Liquid Argon calorimeter, which surrounds the central tracker. The DIS events studied in this paper are triggered on the basis of a scattered electron in the SpaCal, complemented by the signals in the CJCs and multi-wire proportional chambers in the central tracker. Further details of the H1 detector can be found in [8].

2.2 Event Sample

The analysis is carried out using data taken in the years 1996-2000, when HERA collided electrons[1] of energy $27.6\ \mathrm{GeV}$ with protons at $820\ \mathrm{GeV}$ (1996-1997) and $920\ \mathrm{GeV}$ (1998-2000). The integrated luminosity of the sample is $71\ \mathrm{pb}^{-1}$.

The scattered electron energy, measured in the SpaCal, is required to be above $8\ \mathrm{GeV}$, and the virtuality of the exchanged photon[2] is required to lie in the range $5 < Q^2 < 100\ \mathrm{GeV}^2$, as reconstructed from the energy and polar angle of the electron. The DIS SpaCal trigger has a high acceptance for $Q^2 > 5\ \mathrm{GeV}^2$ but had to be prescaled for data below $Q^2 \approx 20\ \mathrm{GeV}^2$ with increasing HERA performance to cope with the inclusive DIS data rate. For $5 < Q^2 < 10$ GeV^2 and $20 < Q^2 < 100\,\mathrm{GeV}^2$ average event weights of 1.25 and 1.03, respectively, have been obtained in this analysis. To ensure that the hadronic final state lies in the central region of the detector, the inelasticity of the event is required to satisfy $0.1 < y < 0.6$, calculated using the scattered electron kinematics. The z coordinate of the event vertex, reconstructed using the central tracker, is required to lie within $35\ \mathrm{cm}$ of the mean position for ep interactions. The difference between the total energy E and the longitudinal component of the total momentum p_z, calculated from the electron and the hadronic final state, is restricted to $35\ \mathrm{GeV} < E - p_z < 70\ \mathrm{GeV}$. This requirement suppresses photoproduction background, where a hadron fakes the electron signature.

The analysis is based on charged tracks reconstructed in the central tracker. Tracks are accepted if they have at least 15 hits in the central jet chambers used for the energy loss measurement and have transverse momenta $p_{\mathrm{T}} > 0.15\ \mathrm{GeV}$ and pseudorapidities in the laboratory frame $|\eta| < 1.75$.

Events are accepted if they contain at least one good measured long-living neutral hadron candidate decaying into two oppositely charged tracks. The candidates have to have a decay vertex with a radial displacement of at least 2 centimetres from the primary interaction point. Furtermore the events have to contain at least one track consistent with originating from the primary vertex.

[1] The analysis uses data from periods when the beam lepton was either a positron (88% of the total) or an electron (12% of the total).

[2] The inclusive DIS kinematic variables are defined as $Q^2 = -q^2$, $y = q \cdot p \,/\, k \cdot p$ and $x = -q^2 \,/\, 2q \cdot p$, where q, k and p are the 4-vectors of the exchanged photon, the incident electron and the incident proton, respectively.

2.3 Selection of K_s^0 Meson and Proton Candidates

The charged decay mode $K_s^0 \to \pi^+\pi^-$ is used to identify K_s^0 mesons. The $\mathrm{d}E/\mathrm{d}x$ measurement for both tracks has to be consistent with the pion hypothesis. For the calculation of the invariant mass, $M(\pi^+\pi^-)$, of each K_s^0 candidate the charged pion mass is assigned to the tracks. Only those K_s^0 candidates having transverse momenta $p_{\mathrm{T}}(K_s^0) \geq 0.3\,\mathrm{GeV}$ and pseudorapidities $|\eta(K_s^0)| \leq 1.5$ in the laboratory frame are accepted for the subsequent analysis. Contamination from Λ and $\overline{\Lambda}$ production is eliminated by requiring the invariant mass under the Λ decay hypothesis to be $M_{p\pi} > 1.121\,\mathrm{GeV}$.

Figure 1 shows the mass distribution for K_s^0 candidates in events with $Q^2 \geq 5\,\mathrm{GeV}^2$. A fit to the data using a sum of two Gaussian functions for the signal and a straight line to approximate the background in the K_s^0 signal region yields $142505 K_S^0$ mesons on a background of 6.6% determined from the $\pm 2\sigma$ region. The peak position is at $M(\pi^+\pi^-) = 496.08 \pm 0.03$ MeV which agrees with the nominal K_s^0 mass $M(K_s^0) = 497.67 \pm 0.03$ MeV [9] within the accuracy of the knowledge of the magnetic field measurement in the central tracking system. Candidate K_s^0 mesons which have a reconstructed $M(\pi^+\pi^-)$ mass within two sigma of the measured K_s^0 mass are selected for the further analysis. The width of the K_s^0 signal depends on the decay topology, which can be “inbening” or “outbending” depending on the orientation of the decay with respect to the magnetic field, resulting in a narrower or a broader resolution of the K_s^0 mass. Therefore a cut of ± 17 and ± 25 MeV is applied for the in- and outbending decay topologies, respectively. The K_s^0 mesons are further combined with tracks originating from the primary vertex.

Figure 2 shows the mass distribution obtained by combining the K_s^0 candidates with a charged track originating from the primary vertex assigned the pion mass. The invariant mass of the $K_s^0\ \pi$ is obtained by fixing the K_s^0 mass to the PDG value. The transverse momentum and pseudorapidity of the $K_s^0\pi$ system are required to be $p_t(K_s^0\pi) > 0.5\ \mathrm{GeV}^2$ and $|\eta(K_s^0\pi)| < 1.5$. The signal from $K^{*\pm}$ production is clearly visible. A fit to the data using a convolution of a Breit-Wigner function with a fixed natural width of 50.9 MeV and a Gaussian together with a background function of the form $\alpha\left(M(K_s^0\pi) - m(K_s^0) - m(\pi)\right)^{\beta} \times \exp\left\{\gamma\left(M(K_s^0\pi) - m(K_s^0) - m(\pi)\right)\right\}$ is performed. The fit yields $18939 K^{*\pm}$ mesons decaying to $K_s^0\pi^\pm$ for $Q^2 \geq 5\,\mathrm{GeV}^2$. The measured peak position $M(K_s^0\pi^\pm) = 890.6 \pm 0.7$ MeV agrees well with the nominal $K^{*\pm}$ mass $M(K^{*\pm}) = 891.66 \pm 0.26$ MeV [9]. The gaussian width of 7.79 ± 2.34 MeV reflects the detector resolution.

Particle identification for these tracks is based on the measured energy loss in the central jet chambers, for details of the $\mathrm{d}E/\mathrm{d}x$ measurement see e.g. [6]. The likelihoods that a particle is a pion, kaon or proton are obtained from the difference between the measured $\mathrm{d}E/\mathrm{d}x$ and the most probable value for each particle type at the reconstructed momentum. The most probable $\mathrm{d}E/\mathrm{d}x$ values are derived from a phenomenological parameterisation [7], which is based on the Bethe-Bloch formula. Particles of a given type $i = \pi, k, p$ are selected via the normalised likelihood LN_i defined to be the ratio of L_i to the sum of the pion, kaon and proton likelihoods.

Proton candidates are selected by requiring $LN_p > 0.3$ for momenta $p(p) < 2$ GeV, which selects protons where they are clearly identified at low momenta and suppresses contributions close to the crossing points of the proton, pion and kaon parameterisations. For $p(p) > 2$ GeV, the requirement is loosened to $LN_p > 0.1$, which suppresses background from particles with large $\mathrm{d}E/\mathrm{d}x$, e.g. electrons.

3 Analysis of $K^0_s\,p$ Combinations

The candidate K^0_s mesons are combined with proton candidates originating from the primary vertex. The invariant mass $M(K^0_s p)$ of these combinations is formed by again fixing the K^0_s mass to its nominal value and for the $K^0_s p$ system $p_t(K^0_s p) > 0.5$ GeV^2 and $|\eta(K^0_s p)| < 1.5$ is required. The $M(K^0_s p)$ distributions for three different bins in Q^2, $5 < Q^2 < 10\,\mathrm{GeV}^2$, $10 < Q^2 < 20\,\mathrm{GeV}^2$ and $20 < Q^2 < 100\,\mathrm{GeV}^2$ are shown in figure 3 together with a fit of a background function of the form $\alpha \cdot (M(K^0_s p) - m(K^0_s) - m(p))^\beta \times \exp\{-(M(K^0_s p) - m(K^0_s) - m(p))) \cdot \gamma\}$ to the data. No significant structure is observed in neither of the Q^2 bins. The experimental resolution of a possible state with zero width decaying to $K^0_s\,p$ is expected to be $\sigma(M(K^0_s p)) = 5$ MeV. The data do not show any indication of a Θ^+ signal. Therefore the $M(K^0_s p)$ distribution is used to set upper limits at 95 % confidence level (C.L.) on the visible Θ^+ production cross section $\sigma(ep \to e\Theta^+ X \to K^0 pX)$. Since the mass of the possible Θ^+ pentaquark is experimentally not well determined, mass dependent limits are derived. In order to set limits, it is assumed that strange pentaquarks are produced by fragmentation and the model described later in this section is used for the determination of efficiencies. The upper limit on the visible cross section is calculated according to

$$\sigma_{u.l.}(ep \to e\Theta^+ X \to K^0 pX) = \frac{N_{u.l.}(M(\Theta^+))}{\mathcal{L}_{int} \cdot \epsilon_{DIS} \cdot \epsilon_{\Theta^+} \cdot BR(K^0 \to K^0_s) \cdot BR(K^0_s \to \pi^+\pi^-)}, \quad (1)$$

where $N_{u.l.}(M(\Theta^+))$, $\mathcal{L}_{int}$, ϵ_{DIS}, ϵ_{Θ^+} and $BR(K^0 \to K^0_s)$, $BR(K^0_s \to \pi^+\pi^-)$ denote the 95% upper limit on the possible number of observed Θ^+ pentaquarks for a given mass $M(\Theta^+)$, the integrated luminosity, the electron acceptance for the visible kinematic range and the Θ^+ selection efficiency from the visible K^0_s and proton range to the visible Θ^+ range including the K^0_s and the proton detection efficiencies as well as the branching ratios for the transition of K^0 to K^0_s and its decay into charged pions. The upper limit on the number of Θ^+ is derived assuming a width of a possible signal of 5 and 8 MeV, using mass windows of ± 10 and ± 16 MeV, respectively.

The acceptances were calculated using the RAPGAP 3.1 [10] event generator incorporating fragmentation according to the Lund string model [11] implemented in PYTHIA 6.2 [12]. For the simulation of the Θ^+ production process, it is assumed that pentaquark production is part of the normal fragmentation process. Therefore the decay of the Θ^+ was introduced by changing the properties of the $\Sigma^{*\pm}$ such that it decays to $K^0_s\,p$ with a natural width of zero and a mass of 1.52 and 1.54 GeV, respectively. This simple model assumes an isotropic decay of the Θ^+ and a production mechanism similar to that of a strange baryon. The generated events are passed through the full detector simulation using GEANT 3.13 [13] and are subsequently subjected to the same reconstruction and analysis chain as data. The acceptances derived from this MC simulation which correspond to low Θ^+ masses of 1.52 to 1.54 GeV will nevertheless be applied to extract mass dependent limits in the mass range from 1.48 to 1.7 GeV.

We consider the following experimental systematic uncertainties on the 95% C.L. upper limit of the Θ^+ production:

- The measurement of luminosity has an uncertainty of 1.5% [14].

- The efficiency of the inclusive DIS event selection, ϵ_{DIS}, has an uncertainty of 13%, which is coming from modeling of the trigger efficiency, the Spacal energy calibration and radiative corrections, as well as systematic effects in the treatment of event weights.
- The efficiency of the $\Theta^+X \rightarrow K_s^0p$ selection, ϵ_{Θ^+}, has an uncertainty of 11% which comprises the uncertainty in modeling track losses (1.8% per track added linearly) and the uncertainty in the efficiency of the $\mathrm{d}E/\mathrm{d}x$ selection (10%).
- The Θ^+ acceptance was estimated from simulated decays at masses of 1.54 and 1.52 GeV. The difference of these two models contributes 3% to the uncertainty. The effect due to the extrapolation of the acceptance derived at masses of 1.52 and 1.54 GeV to higher masses, up to 1.7 GeV, is not considered in this analysis. In addition, the esimate of the efficiency, ϵ_{Θ^+}, has production model dependent uncertainties, which are not considered here since no established production mechanisms for the Θ^+ is known yet.
- The difference in the extracted upper limits using different fitting methods is very small, below 2%. The data were fitted using a background model in the full mass range, excluding the respective mass window and also using the sum of the background function and a gaussian with fixed width and mass to account for a possible signal.

The total systematic uncertainty on the acceptance is 18%.

The resulting upper limits on the visible Θ^+ cross section $\sigma_{u.l.}(ep \rightarrow e\Theta^+X \rightarrow K^0pX)$ at 95% confidence level for different Q^2 bins are shown in figure 4. The full and dashed lines represent the limit using mass windows of ± 10 and ± 16 MeV, respectively. The visible range for Θ^+ production is defined by $5 < Q^2 < 100\,\mathrm{GeV}^2$, $0.1 < y < 0.6$, $pt(K_s^0p) > 0.5\,\mathrm{GeV}$ and $|\eta(K_s^0p)| < 1.5$. In the lowest Q^2 bin an upward fluctuation of the upper limit in the interesting mass region 1.52 to 1.54 GeV is observed. However, a different shape of the fluctuations of the limits for the different Q^2 bins is found. The 95% C.L. upper limits vary between 40 and 120 pb for the different Q^2 regions and over the mass range from 1.48 to 1.7 GeV. The upper limits are also derived for the decay $\Theta^+ \rightarrow K_s^0p$ and its charge conjugate $\Theta^- \rightarrow K_s^0\bar{p}$ separately, shown in 5, which are found to be of compatible size. Fluctuations are observed at different masses for K_s^0p and $K_s^0\bar{p}$ combinations in the shape of the limits.

At high Q^2, $Q^2 \geq 20\,\mathrm{GeV}^2$, positive Θ^+ observation has been reported at a mass of 1.522 GeV by the ZEUS experiment [3]. A visible cross section of Θ^+ production in deep-inelastic scattering at HERA of $\sigma(e^{\pm}p \rightarrow e^{\pm}\Theta^+X \rightarrow e^{\pm}K^0pX) = 125 \pm 27(stat.)^{+36}_{-28}(syst.)$ pb in the kinematic range $Q^2 > 20\,\mathrm{GeV}^2$, $0.04 < y < 0.95$, $p_t(\Theta^+) > 0.5$ and $|\eta(\Theta^+)| < 1.5$ was observed [16] using a data sample with an integrated luminosity of 121 pb^{-1}. The K_s^0p system was reconstructed using a different method for the proton identification than in the analysis presented here. Only low momentum protons, $p(p) < 1.5\,\mathrm{GeV}$ are selected and a visual selection of bands in the $\mathrm{d}E/\mathrm{d}x$-p plane is used [3]. In order to be able to compare the upper limits on the Θ^+ production more directly to these results, the analysis described above was repeated using a selection more similar to that used in [3], in the following called "low momentum $\mathrm{d}E/\mathrm{d}x$ selection". The $\mathrm{d}E/\mathrm{d}x$-likelihood proton selection was replaced by a visual selection, requiring $\mathrm{d}E/\mathrm{d}x > 1.15$, $p(p) < 1.5$ GeV and $f_1 < \mathrm{d}E/\mathrm{d}x < f_2$, where f_i are functions following the parameterization of the most probable $\mathrm{d}E/\mathrm{d}x$ values but shifted according to the $\mathrm{d}E/\mathrm{d}x$ resolution in order to enclose 98 % of the proton band. The resulting invariant $K_s^0p(\bar{p})$ mass spectra are shown in figure 6 for the highest Q^2 bin, $20 < Q^2 < 100\,\mathrm{GeV}^2$, for all combinations (upper left plot) as well as for the $K_s^0 p$ and $K_s^0 \bar{p}$ combinations separately (lower left and lower right plot). Also for this low momentum $\mathrm{d}E/\mathrm{d}x$ selection no significant signal could be found. The upper limits on the Θ^+ cross section at 95 % confidence level derived from these mass spectra are shown in figure 7 for all combinations and in figure 8 for the positive (top) and negative (bottom) combinations. Around the mass of 1.52 GeV an upper limit on the cross section of roughly 100 pb is found, which does not exclude the cross section observed by the ZEUS experiment.

4 Conclusions

The preliminary results of the search for the strange pentaquark Θ^+ in deep inelastic ep scattering has been presented. No significant signal for Θ^+ production in its possible decay mode $\Theta^+ \to K_s^0 p$ has been observed in the $K_s^0\, p$ mass distribution for different regions in Q^2 between 5 and 100 GeV^2. With the assumption that pentaquarks are produced by fragmentation $K_s^0\, p$ mass dependent upper limits on the cross section $\sigma(ep \to e\Theta^+ X \to K^0 p(\bar{p})X)$ are derived as a function of Q^2 and found to vary between 40 and 120 pb over the mass range of 1.48 to 1.7 GeV.

In order to compare to the previous measurement of the visible Θ^+ cross section by the ZEUS collaboration, the analysis was repeated with a low momentum $\mathrm{d}E/\mathrm{d}x$ selection. The resulting upper limit does not exclude the previosly observed cross section [16]. The present statistical precision in the HERA I data sample is not sufficient to draw a stronger conclusion.

References

[1] T. Nakano *et al.*, (LEPS), Phys. Rev. Lett. **91** (2003) 012002;
S. Stepanyan *et al.*, (CLAS), Phys. Atom. Nuclei **66**, 1715 (2003);
J. Barth *et al.*, (SAPHIR), Phys. Lett. B **572** (2003) 127;
V. Kubarovsky *et al.*, (CLAS), Phys. Rev. Lett. **92** (2004) 03201 [erratum-ibid. 92 (2004) 049902].

[2] V. V. Barnim *et al.*, (DIANA), Phys. Atom. Nucl. **66** (2003) 1715 [Yad. Fiz. 66 (2003) 1763];
A. E. Asratyan, A. G. Dolgolenko and M. A. Kubantsev, Phys. Atom. Nucl. **67** (2004) 682;
A. Aleev *et al.*, (SVD), hep-ex/0401024;
A. Airapetian *et al.*, (HERMES), Phys. Lett. B **585** (2004) 213;
M. Abdel-Bary *et al.*, (COSY-TOF),Phys. Lett. B **595** (2004) 127;

[3] S. Chekanov *et al.* [ZEUS Collaboration], Phys. Lett. **591** (2004) 7.

[4] J. Z. Bai *et al.*, (BES), Phys. Rev. D **70** (2004) 012004;
BaBar Collaboration, hep-ex/0408064;
BELLE Collaboration, hep-ex/0409010;
S. R. Armstrong, hep-ex/0410080; S. Schael *et al.*, (ALPEH), Phys. Lett. B **599**(2004) 1;
I. Abt *et al.*, (HERA-B), Phys. Rev. Lett. **93** (2003) 212003;
Yu. M. Antipov *et al.*, (SPHINX), Eur. Phys. J. A **21**, 455 (2004);
M. J. Longo *et al.*, (HyperCP), Phys. Rev. D **70** (2004) 111101;
D. O. Litvintsev, (CDF), hep-ex/0410024;
R. Mizuk *et al.*, (Belle), hep-ex/0411005;
C. Pinkerton *et al.*, (PHENIX), J. Phys. G **30** (2004) 1201;
R. De Vita, (CLAS Collaboration), *Search for pentaquarks at CLAS in photoproduction from protons*,American Physical Society Meeting, Tampa, Florida, April 2005;
C. Risler, (H1), *H1 Search for a Narrow Baryonic Resonance Decaying to* $K_s^0 p(barp)$ presented at DIS2005, Madison, Wisconsin, Spring 2005.

[5] R. Jaffe, SLAC-PUB-1774, talk presented at the Topical Conf. on Baryon Resonances, Oxford, UK, 1976;
H. Høgaasen and P. Sorba, Nucl. Phys. B **145** (1978) 119;
D. Strottman, Phys. Rev. **D20** (1979) 748;
C. Roisnel, Phys. Rev. **D20** (1979) 1646.
D. Diakonov, V. Petrov and M. V. Polyakov, Z. Phys. **A359** (1997) 305 [hep-ph/9703373].
R. L. Jaffe and F. Wilczek, Phys. Rev. Lett. **91** (2003) 232003 [hep-ph/0307341].
H. Walliser and V. B. Kopeliovich, [Zh. Eksp. Teor. Fiz. **124** (2003) 483] [hep-ph/0304058];
S. Capstick, P. R. Page and W. Roberts, Phys. Lett. **B570** (2003) 185 [hep-ph/0307019];
M. Karliner and H. Lipkin, Phys. Lett. **B575** (2003) 249 [hep-ph/0402260];
D. E. Kahana and S. H. Kahana, [hep-ph/0310026];
E. Shuryak and I. Zahed, [hep-ph/0310270].

[6] A.Aktas *et al.* [H1 Collaboration] Phys. Lett **B 588** (2004) 17.

[7] J. Steinhart, 'Die Messung des totalen $c\bar{c}$-Photoproduktions-Wirkungsquerschnittes durch die Rekonstruktion von Λ_c Baryonen unter Verwendung der verbesserten $\mathrm{d}E/\mathrm{d}x$ Teilchenidentifikation am H1 Experiment bei HERA', Ph.D. thesis, 1999, Universität Hamburg (in German, available from
`http://www-h1.desy.de/publications/theses_list.html`).

[8] I. Abt *et al.* [H1 Collaboration], Nucl. Inst. Meth. **A386** (1997) 310;
I. Abt *et al.* [H1 Collaboration], Nucl. Inst. Meth. **A386** (1997) 348.

[9] Particle Data Group, H. Hagiwara *et al.*, Phys. Rev. **D66** (2002) 010001.

[10] H. Jung, Comp. Phys. Comm. **71**, 15 (1992).

[11] B. Andersson, G. Gustafson, G. Ingelman and T. Sjöstrand, Phys. Rept. **97** (1983) 31.

[12] T. Sjöstrand *et al.*, Comp. Phys. Commun. **135** (2001) 238 [hep-ph/0010017].

[13] R. Brun *et al.*, GEANT3, Technical Report CERN-DD/EE/84-1, CERN, 1987.

[14] H1 Collaboration, *Luminosity Measurement in the H1 Experiment at HERA*, In Proceedings of the International Conference on High Energy Physics pages 17-26, DESY, 1996.

[15] U. Bassler, G. Bernardi, *Structure function measurements and kinematic reconstruction at HERA*, Nucl. Instr. and Meth. **A426** (1998) 583.

[16] S. Chekanov *et al.* [ZEUS Collaboration], *Cross section measurements of a narrow baryonic state decaying to $K_s^0 p$ and $K_s^0 \bar{p}$ in deep inelastic scattering at HERA*, Contributed paper to 32nd International Conference on High-Energy Physics, Beijing(2004), abstract no. 10-0273.

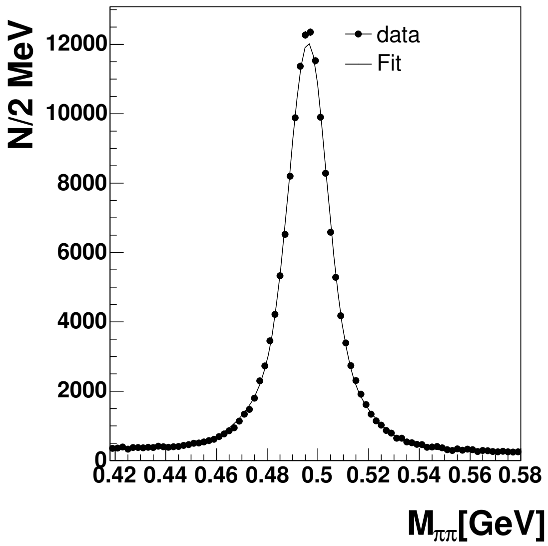

Figure 1: Inclusive K_S^0 signal for $Q^2 > 5\text{GeV}^2$. We observe $142505 K_S^0$ at a mass of $M = 496.08 \pm 0.03$ MeV using a linear fit describing the background and two gaussians to account for the signal.

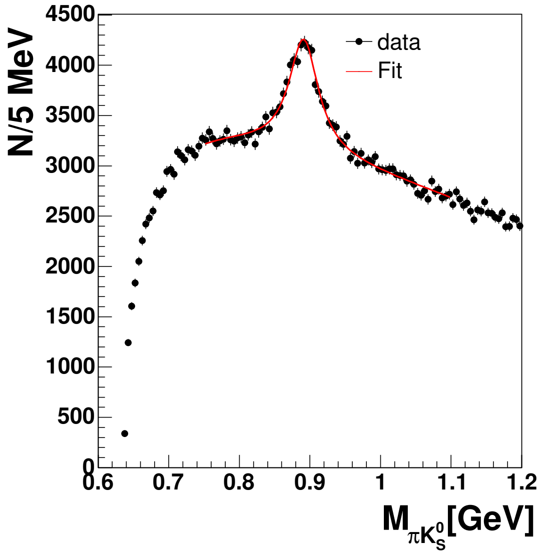

Figure 2: Inclusive K^* signal for $Q^2 > 5\text{GeV}^2$. The signal is fitted by a convolution of a Breit-Wigner function with a fixed natural width of 50.9 MeV [9] and a gaussian. We observe $18939 K^*$ at a mass of $M = 890.6 \pm 0.7$ GeV. The gaussian width of 7.79 ± 2.34 MeV reflects the detector resolution.

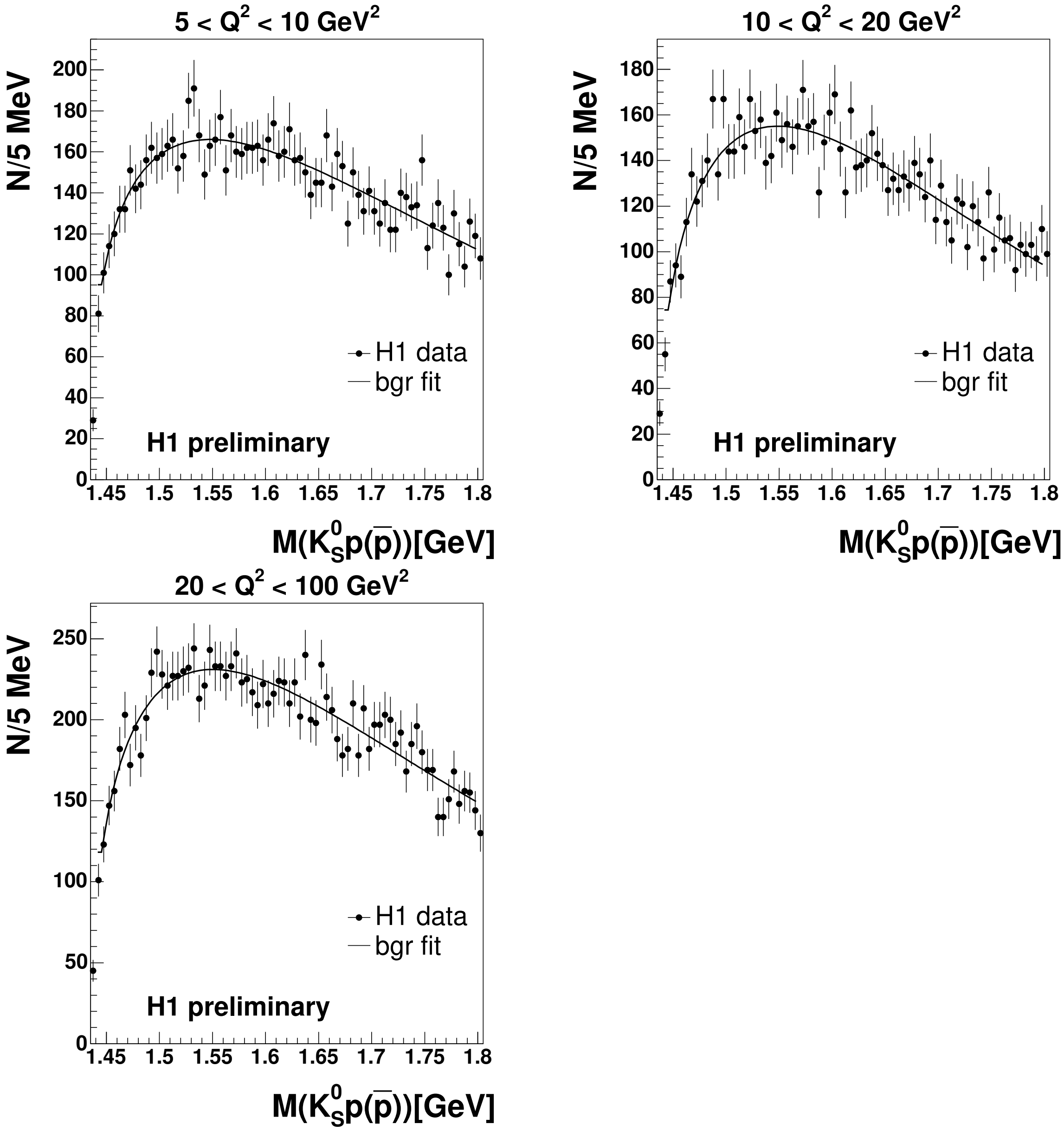

Figure 3: Invariant $K^0_S p(\bar{p})$ mass spectra for the standard dE/dx selection in bins of Q^2, which are used for the limit extraction. The full line shows the result from the fit of a background function to the data. The mass spectra show upward fluctuations at different masses but no significant peak is observed.

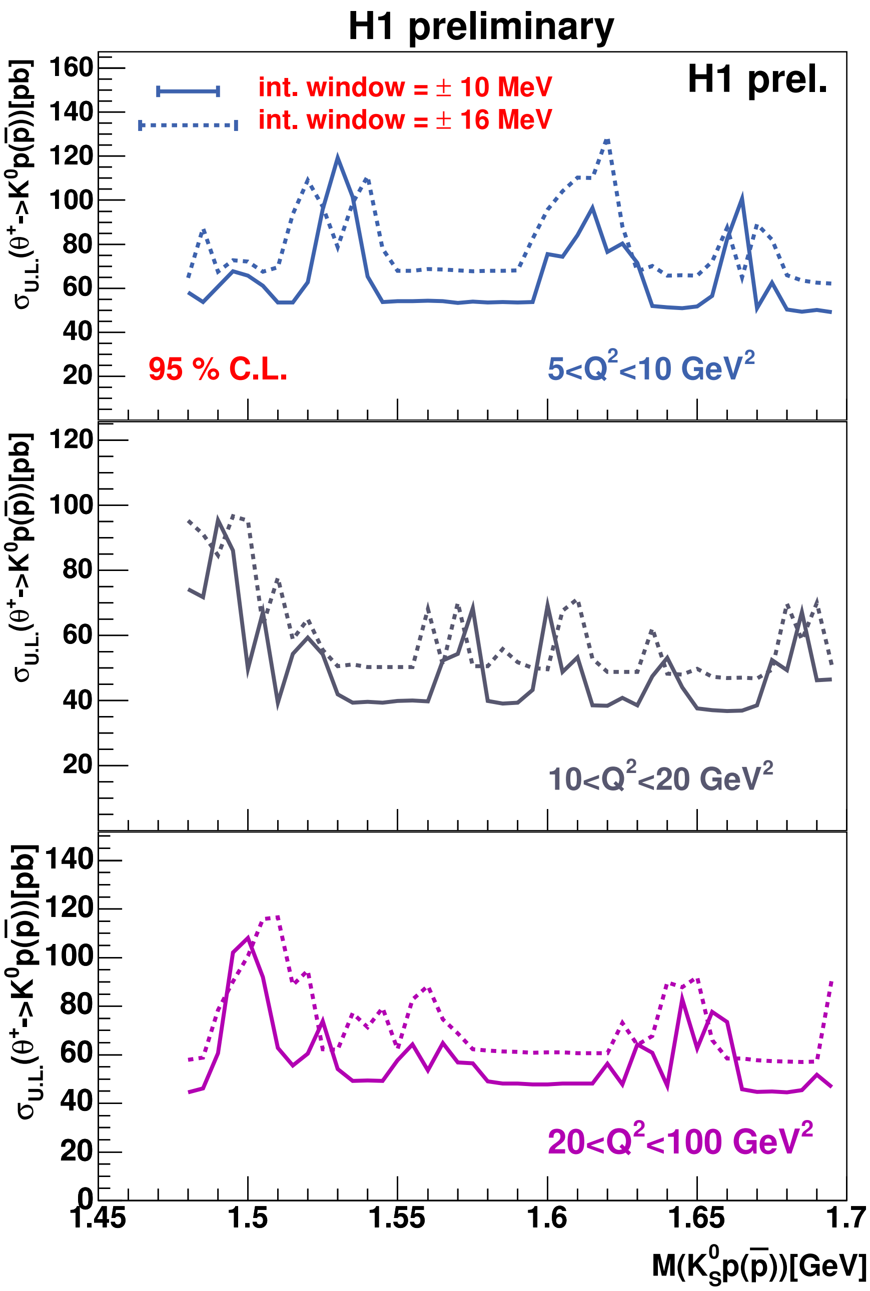

Figure 4: Upper limits on the cross section $\sigma_{U.L.}(ep \to e\theta^+X \to eK^0p(\bar{p})X)$ at 95% confidence level in bins of Q^2 in the visible range $p_T(K_s^0p) > 0.5$ GeV and $|\eta(K_S^0p)| < 1.5$. The full and dashed line represents the limit using ± 10 and ± 16 MeV mass windows, respectively.

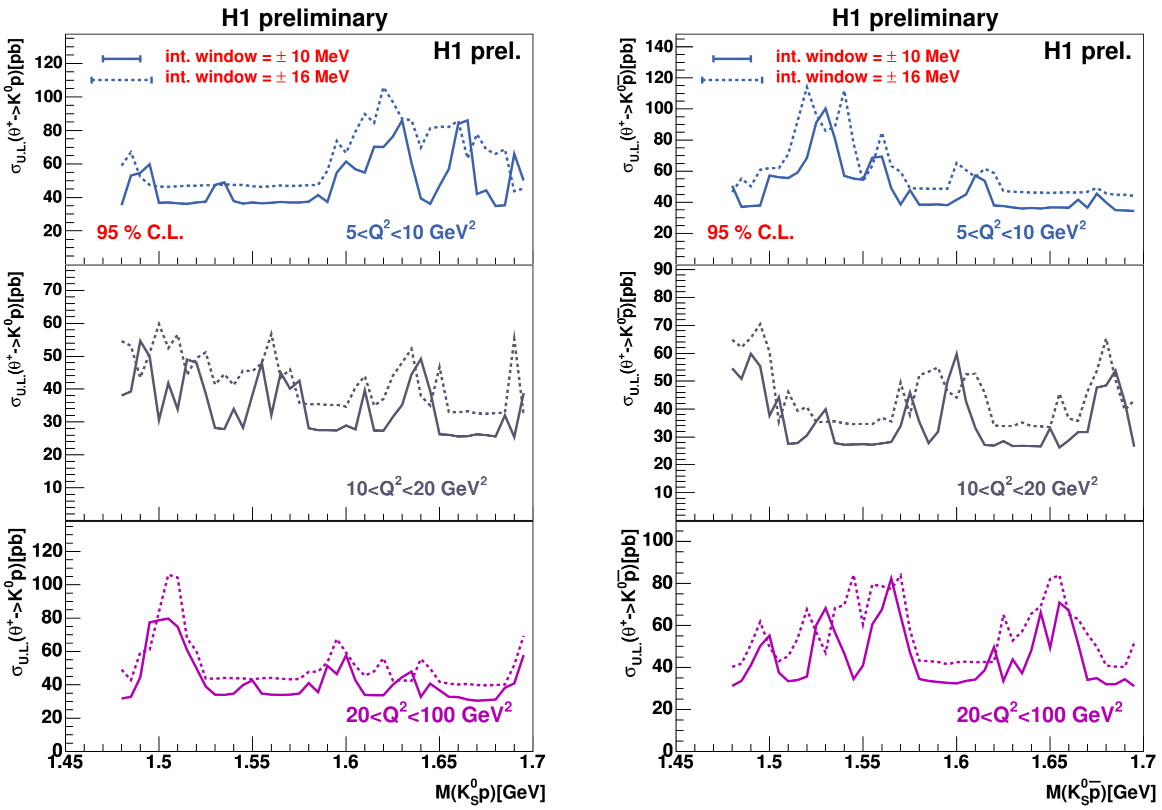

Figure 5: Upper limits on the cross section $\sigma_{U.L.}(ep \to e\theta^+X \to eK^0pX)$ at 95% confidence level in bins of Q^2 for K_s^0p (left) and $K_s^0\bar{p}$ (right) separately.

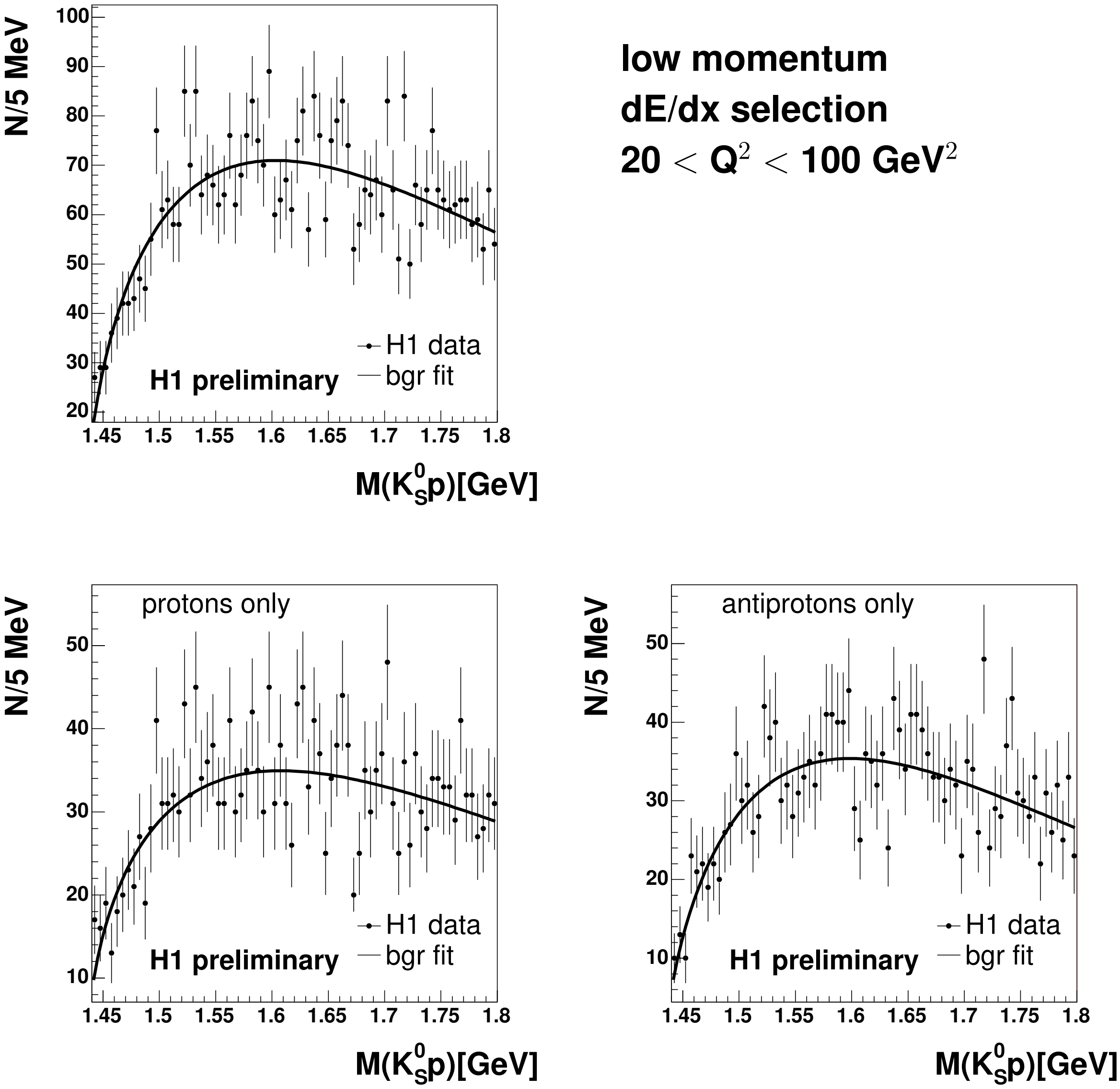

Figure 6: Invariant $K_S^0 p$ mass spectra in the highest Q^2 bin, $20 < Q^2 < 100\ \mathrm{GeV}^2$, for the low momentum dE/dx selection, where instead of likelihoods a visual dE/dx selection and an upper momentum cut $p(p) < 1.5$ GeV is applied. The upper left plot shows the invariant mass for $K_s^0 p$ and $K_s^0 \bar{p}$ combinations, the lower left and right plot the mass spectra separately for the positive and negative combinations, respectively.

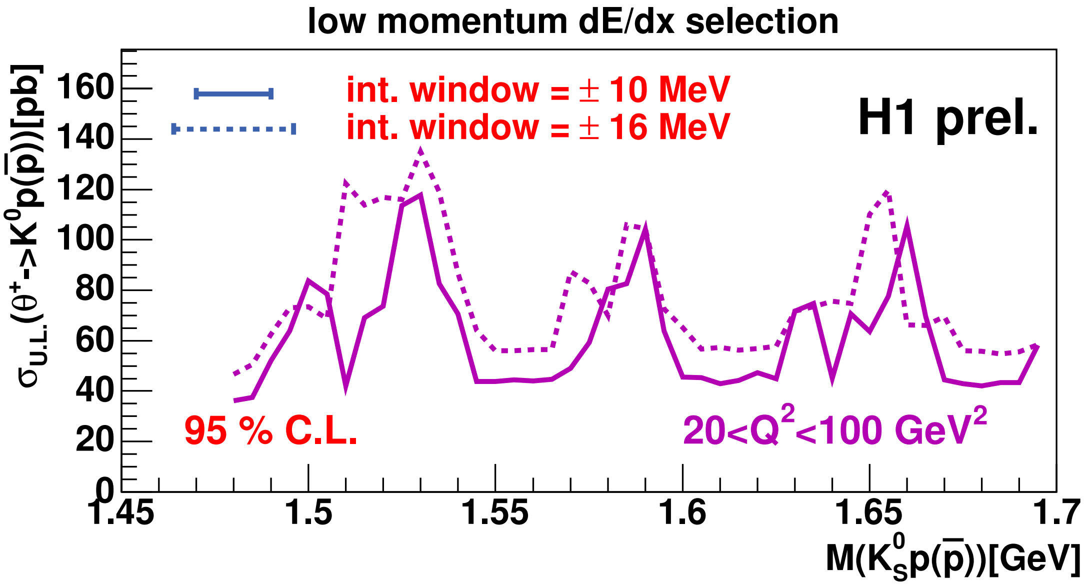

Figure 7: Upper limits on the cross section $\sigma_{U.L.}(ep \rightarrow e\theta^{+}X \rightarrow eK^{0}p(\bar{p})X)$ at 95% confidence level for $20 < Q^2 < 100\ \text{GeV}^2$ using the low momentum $\mathrm{d}E/\mathrm{d}x$ selection.

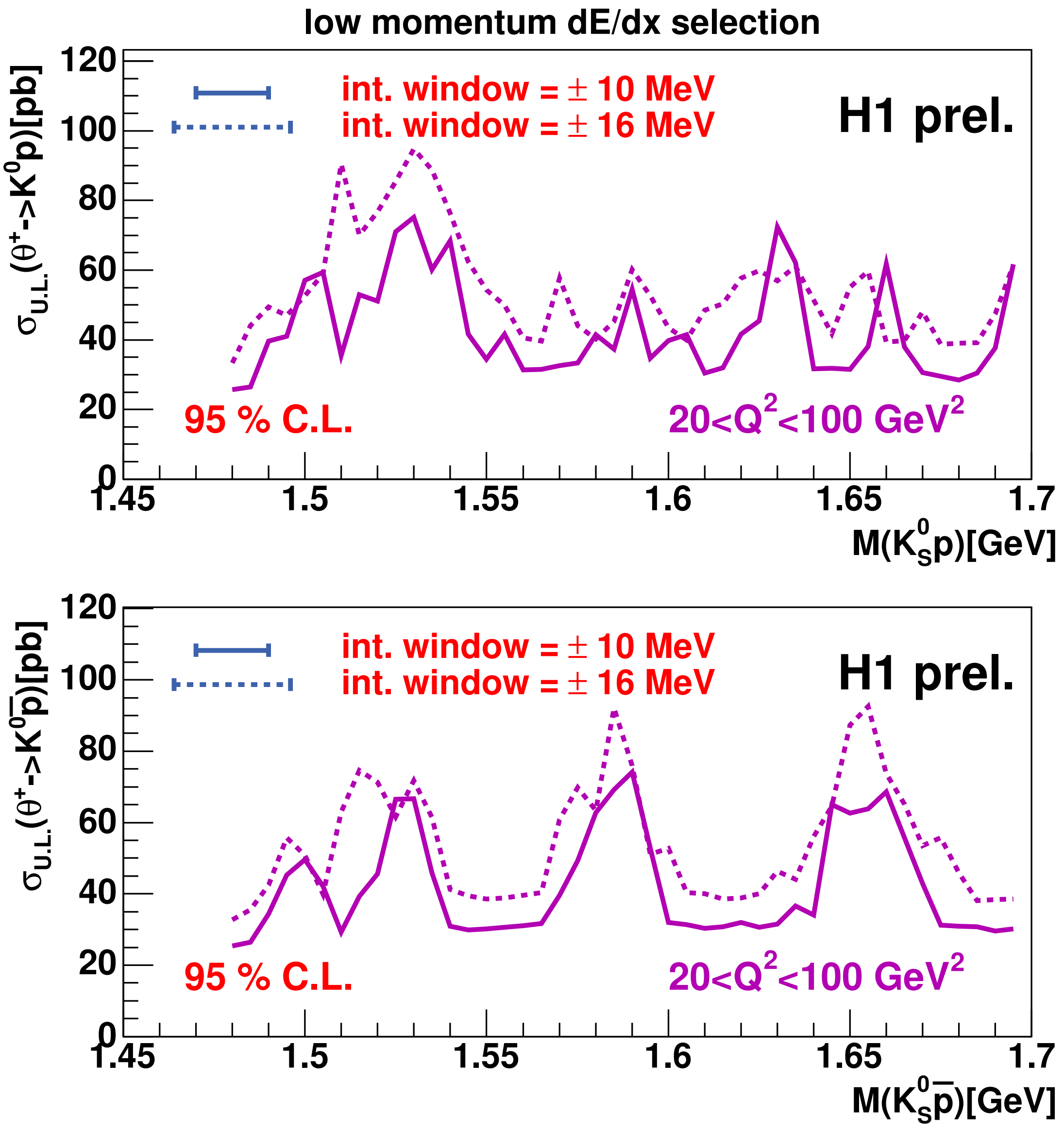

Figure 8: Upper limits on the cross section $\sigma_{U.L.}(ep \rightarrow e\theta^+X \rightarrow eK^0p(\bar{p})X)$ at 95% confidence level for $20 < Q^2 < 100\ \mathrm{GeV}^2$ using the low momentum $\mathrm{d}E/\mathrm{d}x$ selection for $K^0_s p$ (top) and $K^0_S\bar{p}$ (bottom), separately.